International Journal of Computer Information Systems and Industrial Management Applications
ISSN 2150-7988 Volume 18 (2026) pp. 1–17

https://doi.org/10.70917/ijcisim-2026-0209
Article

Coupling Mechanism of Intelligent Optimization Design of TMD Parameters of Bidirectional Dense Rib Cavity Building Cover with BIM Technology Application in Enterprises and the Path to Improvement of Operational Efficiency

Jianyong Chen*

* Wuhan Technical University, Wuhan, Hubei, 430000, China; Chenjywtc@163.com

Abstract: Traditional vibration-resistant methods have limitations and cannot effectively suppress structural vibration, which may jeopardize the safety of building construction and reduce the operational efficiency of building construction. The article combines BIM technology with the optimal design of TMD parameters of two-way dense ribbed cavity building cover, designs a horizontal omnidirectional TMD device, and introduces genetic algorithm to obtain the optimal TMD parameters. After considering the flutter uncertainty, a case study is carried out based on the two-way dense-ribbed cavity building model constructed by BIM technology. The results show that the flutter vibration control efficiency can reach up to 45.15%, and the longitudinal root-mean-square (RMS) vibration reduction rate of HO-TMD is 15.37% while realizing active frequency modulation. In engineering practice, the introduction of BIM technology can help establish an accurate bidirectional dense-ribbed cavity building cover, which makes the optimized design of TMD parameters more targeted and improves the safety of building construction and operational efficiency.

Keywords: TMD; BIM; flutter uncertainty; bi-directional dense-ribbed cavity building cover

1. Introduction

As an important part of the building structure, the building cover plays the role of bearing the top and bottom, the building cover through the beams and columns will be applied to the load applied to the vertical load-bearing structure, and ultimately the load applied to the foundation [1]. The building cover is the direct load bearing body of vertical loads, playing the role of isolating space, ensuring the stability of walls and columns, and transferring loads [2]. The building cover and beams and columns are combined with each other and work together to form a reasonable force system [3]. The building cover comes into being along with the development of the building, and with the rapid development of the construction industry, the material composition, structural form and construction technology of the building cover undergoes great changes. On the one hand, considering the requirements of environmental protection, people's desire for green materials has become stronger and stronger [4]. On the other hand, under the premise that concrete material remains unchanged, the adoption of reasonable cross-sectional form of the building cover can effectively solve the people's requirements for the beautiful appearance of the building and the variety of internal functions [5-7]. The building cover structure of the traditional building cover structure (the concrete material is the same) It is because the traditional floor cover structure (beam floor cover and beamless floor cover) can no longer adapt to the current needs of people in terms of architectural function, construction technology and other aspects. In

order to adapt to the pace of the times and meet people's needs, researchers and engineers have invented several new types of building cover structures on the basis of hollow core building covers.

Two-way dense-ribbed cavity floor cover is an update and expansion on the basis of the structural system of beamless floor cover, and the two-way dense-ribbed cavity floor cover consists of hollow box and cast-in-situ reinforced concrete dense-ribbed beams. The beam spacing of two-way dense-ribbed cavity floor cover is small and positively crossed, so it not only has good force performance, large stiffness, small deflection, but also has good overall performance, while the overall cost is relatively low [8-11]. Currently, bi-directional dense-ribbed cavity floor cover is widely used in various types of large-span and large-loaded building structures. Ma, J et al. (2022) proposed a digital design and construction process for the dense-ribbed cavity floor cover system, which is in the bi-directionally evolving structural optimization framework, generating the building structure with continuous rib layout and higher structural stiffness. In a two-way evolutionary structural optimization framework, a floor slab design with continuous rib layout and higher structural stiffness was generated, and the structural stiffness and sustainability were improved by topology optimization and 3D printing of complex shaped column formwork [12]. Huang, Y et al. (2022) proposed a new bi-directional dense-ribbed cavity floor structure with permanent infill (BDF grid steel box). It exhibits a very high bi-directional vertical load carrying capacity and has been shown through experimental and simulation results that the integration of three unidirectional precast panels into a single bi-directional floor structure can be realized to support the building as a whole [13]. Bosbach, S et al. (2023), in order to reduce resource consumption and carbon emissions in the construction industry, proposed the use of corrosion-resistant carbon fiber-reinforced polymer (CFRP) reinforcing bars made of a new type of ribbed ribbed floor slabs and provided a lightweight structural system that significantly reduces deadweight and is suitable for dense ribbed cavity floor slabs [14].

Souza, C et al. (2020) found that gypsum ceilings with a resilient layer under a stucco plaster layer were able to reduce the weighted impact sound pressure level of unidirectional ribbed and hollow brick panels by 41 dB , the results of this study were carried out in a controlled vertical acoustic resonance chamber complying with International Organization for Standardization (ISO) standards, which can be used as a reference for the structural optimization of dense-ribbed cavity floor coverings [15]. Mata-Falcón, J et al. (2022) found that the use of a digital process to manufacture ribbed concrete floor covers is able to reduce the amount of concrete used by approximately 50% compared to the manufacture of solid floor slabs, while at the same time the current process is still wasteful and labor-intensive problems, which need to be further optimized and improved for sustainable development [16]. Chen, X and Ma, Q (2024) investigated the cavity concrete composite floor cover which is tightly connected and has no protruding reinforcement inside, and found that it has the same flexural performance as the non-spliced slab under normal conditions, but under extreme conditions it may problems such as joint failure may occur, while its bidirectional load carrying capacity can be enhanced by adding reinforcement [17]. Jin, J et al. (2025) constructed a new bi-directional dense-ribbed cavity floor slab, which ensures that the bi-directional force characteristics and assembly efficiency can be significantly improved without decreasing the unidirectional structural performance, and this result has been proved by experimental and numerical studies [18]. Zhang, Z et al. (2025) investigated the mechanical properties and failure mechanism of large-span, cast-in-place cavity-core-molded concrete floor covers under vertical loading, and derived from field tests and numerical simulations that their ultimate bearing capacity was 27.2 kN/m^2 and is always in the elastic range under vertical loading [19]. So far, although theoretical calculation methods and construction principles have been proposed by theoretical analysis and finite element analysis, and corresponding experimental studies have been made on the dense ribbed cavity floor cover structure, most of these analyses and studies focus on the local components of the dense ribbed cavity floor cover structure under static load, and the overall floor cover structure under seismic action has not been studied. However, most of these analyzes and researches focus on the local components of dense-ribbed hollow-cavity building structures under static load, and there are relatively few researches on the mechanism and damage pattern of the whole building structure under earthquake.

Tuned mass damper (TMD), as a technical method of vibration control, has laid a solid foundation for the later research on vibration control of TMD architecture by domestic and foreign scholars [20-21]. For the optimization of TMD parameters, Islam, B and Ahsan, R (2012) aimed at minimizing the dynamic parameters of the TMD system, and through the numerical global optimization (EVOP) algorithm was simulated for the response of the structural system, enabling a more rational selection of the TMD parameters [22]. Farshidianfar, A and Soheili, S (2013) used the artificial bee colony (ABC) algorithm to optimize the TMD parameters, which takes the TMD mass, damping coefficients and spring stiffness as design variables with the aim of reducing the maximum displacements and accelerations of the building and thus mitigating the seismic oscillations [23]. Kamgar, R et al. (2018)

proposed an optimal design of TMD for seismic vibration control for structures subjected to critical earthquakes with the objective of minimizing roof displacement and demonstrated that the scheme is not only effective in reducing the roof displacement, but also significantly improve the seismic performance of the building [24].Kaveh, A et al. (2020) used the Chaotic Optimization Algorithm (COA) to optimize the parameters of the TMD system, and the numerical results showed that the optimal parameters of the TMD provided by this scheme have good attenuation ability under different excitations for the structural system response [25]. Djedoui, N and Ounis, A (2022) detailed the Gray Wolf Optimization Algorithm (GWO) , Moth Flame Optimization Algorithm (MFO) and Whale Optimization Algorithm (WOA) Three meta-heuristic optimization algorithms were applied in TMD parameter optimization while considering the soil-structure interaction (SSI) effect in the frequency domain, and it was found that the GWO algorithm was able to reach the optimal solution faster and more efficiently [26] .Suryadi, D et al. (2023) optimized the TMD parameters by using genetic algorithm and simulation results showed that the optimum ratios were 10% for mass, 10% for stiffness and 1% for damping. where the seismic response was reduced by 85.94% and the vibration amplitude was significantly reduced from 0.24259 m to 0.034385 m [27]. Yang, X et al. (2023) used machine learning to optimize the design of TMD parameters and found that Generative Adversarial Networks (GAN) can guide the evolution of the parameters to obtain newer parameters, while a better set of parameters can also be identified through multi-objective optimization and a Pareto optimal solution can be obtained [28].

Aiming at the current problem of not being able to take into account the vibration damping effect of two-way dense-ribbed cavity building cover, this paper proposes a TMD parameter optimization design method combined with BIM technology. Based on the two-way dense-ribbed cavity building cover model established by BIM technology, the method designs a horizontal omni-directional TMD device with full consideration of the uncertainty of vibration, and introduces a genetic algorithm to obtain the optimal TMD parameters. This method can effectively improve the vibration damping effect of two-way dense-ribbed cavity building cover, and fully ensure the stability of two-way dense-ribbed cavity building cover in practical engineering applications.

2. BIM-based modeling of bi-directional dense-ribbed cavity building cover

The rapid evolution of the new era has led to the continuous development and improvement of the economy, which makes people's requirements for the use of buildings and their safety higher and higher. In addition, there are more and more high-rise buildings nowadays, which have higher requirements on the seismic performance and stability of the structure. Therefore, the study of vibration damping of two-way dense-ribbed cavity building cover is of great significance to a certain extent.

2.1. Two-way dense-ribbed cavity building with BIM technology

2.1.1. Two-way dense-ribbed cavity building

The bidirectional dense-ribbed cavity floor cover studied in this paper is composed of precast concrete base slab, precast cavity members, precast steel reinforcement skeleton, post-cast rib beams and panels (post-cast laminated layer). The cavity inner mold and the prefabricated part of the stacked plate are integrated into one in the factory for large-scale production, and a certain width of gap is reserved between the boxes of the prefabricated base plate and the reinforcement is pre-buried to form the longitudinal and transversal dense ribs, and the plate is transported to the construction site and installed in place for the second casting to form a two-way dense ribbed cavity floor slab with good integrality. The cavity members consist of cementitious materials that bond well to concrete and are available in a variety of forms. It can be a closed hexahedron or a pentahedron with openings on the bottom surface, which is hollow inside, or it can be filled with partially or completely lightweight material, and the cavity member selected in the BIM model for this study is a pentahedron with openings on the bottom surface.

The precast base plate of this two-way dense ribbed cavity floor cover acts as a formwork in the later pouring process, and after the concrete is poured, a two-way dense ribbed cavity floor cover with two-way stress is formed. It has the advantages of saving formwork, saving concrete, saving time and labor, and the overall structural performance is good, and the cross-section height of structural components is small, which can reduce the building height or increase the building headroom. It can also reduce the deadweight, reduce the floor height, and reduce the comprehensive cost.

2.1.2. BIM Technology Basics

Building Information Modeling (BIM) is to digitize the information of a building project as a way of expression, to establish a 3D model of the virtual building, to simulate the real situation by integrating all kinds of information and data through the model, and to form the information sharing and transmission in the whole cycle of the project, such as planning, designing, producing, constructing, operating, and so on. It is convenient for owners, designers, component manufacturers, constructors, operators, etc. to use, update, and correct the information to form the collaborative work of each participant.

Among them, the concept of BIM mainly contains three aspects:

(1) BIM is a model of multi-dimensional information integration technology that collects data on relevant project information and expresses the physical situation and functional requirements of the project using digital technology.

(2) BIM is a model that integrates data and resources at all stages of the project cycle, and the data can be calculated, found, and combined at any time, and the data and resources can be used by all parties involved in the construction.

(3) BIM is a platform for sharing resources, which can solve the problem of decentralization and the unity of different kinds of data, and can enable the dynamic creation, management and sharing of project information, which can provide a basis for the work of decision makers [29].

2.2. BIM-based modeling of bi-directional dense-ribbed cavity building cover

2.2.1. Parametric component library creation

Parametric component database is the technical cornerstone for realizing intelligent analysis of engineering quantity. Based on the requirements of engineering practice and following the principle of component taxonomy, the building entity is divided into beams, slabs, columns and other basic units and clusters of composite components. Relying on the family editor function of mainstream BIM platforms (e.g. Revit, Bentley), the geometric topological parameters (length, width, height, positioning coordinates) and non-geometric attribute parameters (concrete strength level, node construction practices) of the components are defined, and heterogeneous data integration is realized through the IFC standard. In order to ensure the industrial adaptability of the database, it is necessary to strictly refer to the national standards for parameter coding, and establish component version control and semantic association rules. Eventually, a component resource management system based on semantic web technology is constructed to realize multi-dimensional retrieval of components, iterative tracking of versions and analysis of cross-project reuse rate, and to ensure the consistency of data between the database and the project volume when design changes are made.

At the level of parameterized configuration, each component family integrates 15 core attribute parameters, including wall thickness tolerance, axial extension, flange sealing form and other key design variables, relying on the parameter-driven characteristics of the Revit platform to realize the dynamic interactive adjustment of attribute parameters at the design stage.

For the spatial interference problem in the construction stage, the intelligent conflict avoidance mechanism is embedded in the component library, and by presetting the minimum safe clear distance threshold (e.g., the distance between the contact surface and the concrete beam ≥40mm), combined with the real-time collision check function of the Navisworks platform, collision detection is carried out for all the specialties of the model, forming the closed-loop management and control system of "Parameter Setting - Collision Warning - Positioning Correction The closed-loop control process of “parameter setting - collision warning - positioning correction” is formed.

2.2.2. Main structure modeling

Combined with the previous BIM application experience and the demand for BIM application of the hollow core building cover, the model accuracy is determined to be LOD450, i.e. the depth of the construction model, and the model is refined to the components, with accurate appearance, size and material to meet the needs of processing and simulation, and the basic information is entered completely, which facilitates the extraction of engineering quantities.

Use BIM model and simulation to determine the specific size of the steel mesh box to ensure the quality of processing and installation. Processing of semi-finished products (galvanized steel sheet forming, internal supporting steel skeleton) according to BIM model in the rear processing yard, and on-site assembling and welding. The processing of the box mesh is completed through the automation of special machinery for rapid punching and cutting, pressing and tensioning, positioning and cutting, and sizing and creasing. The endoskeleton is trihedral, the upper mesh plate is bent and closed, and the corresponding specification of blocking mesh plate is placed at both ends [30].

The bidirectional dense-ribbed cavity floor cover mold frame as the cavity floor cover steel, concrete construction of the precondition, the model quality also directly affects the building cover BIM application, so the mold frame is also LOD450 modeling, for the reinforcement, steel mesh box installation, concrete pouring simulation, etc., to provide a basic reference. After the model is established, the model is used to carry out the three-dimensional layout of the steel mesh box, and the layout is carried out according to the four weeks to the middle, and the non-standard plate is set up in the span of the plate according to the actual size to determine the size specification and quantity of the steel mesh box.

3. Optimized design of TMD parameters considering chattering

Horizontal forces on the building structure need to be transmitted and resisted by corresponding members, and the building cover, as a horizontally stressed member, has a weak tensile capacity of reinforced concrete structure when it is not supported by supporting structural columns. Therefore, a two-way dense ribbed cavity building cover model is established based on BIM technology, and the parameters of the tuned mass damper (TMD) installed in the cavity building cover are optimized to enhance the stability of the two-way dense ribbed cavity building cover and ensure the safety of the building based on the consideration of the flutter uncertainty of the building cover.

3.1. TMD damping principle and quantification of flutter uncertainty

3.1.1. TMD Damping Vibration Model

Tuned mass damper (TMD) as a control method for passive vibration damping is widely used in the fields of buildings and bridges [31]. The principle of TMD damping is to suppress the vibration of the main system by attaching the TMD damping device to the main system, and transferring the vibration energy of the main system to the TMD for energy dissipation through the precise tuning function. The forced vibration model is shown in Fig. 1, and the TMD damping system can be simplified as a two-degree-of-freedom damped vibration system.

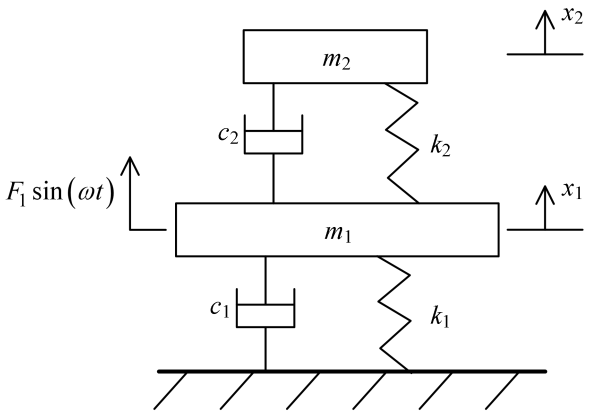

Figure 1. Forced vibration model of a two-degree-of-freedom system

In the figure, m_1, m_2 is the mass of the main system and the TMD, respectively, k_1, k_2 is the stiffness of the main system and the TMD, respectively, c_1, c_2 is the damping of the main system and the TMD, respectively, x_1, x_2 is the displacement of the main system and the TMD with respect to the ground, respectively, $F_1\sin(\omega t)$ is the forcing force on the main system, ω is the excitation angular frequency, and F_1 is the excitation amplitude.

The forced vibration equation of the system is:

$$\begin{cases} m_1\ddot{x}_1 + (c_1 + c_2)\dot{x}_1 - c_2\dot{x}_2 + (k_1 + k_2)x_1 - k_2x_2 = F_1\sin(\omega t) \\ m_2\ddot{x}_2 + c_2(\dot{x}_2 - \dot{x}_1) + k_2(x_2 - x_1) = 0 \end{cases} \tag{1}$$

The solution of the vibration equation is dimensionless and the vibration response of the master system is obtained as:

$$\left|\frac{X_1}{\delta_{\mathrm{st}}}\right| = \sqrt{\frac{A^2+B^2}{C^2+D^2}} \tag{2}$$

where:

$$\begin{cases} A = 2\xi g \\ B = g^2 - f^2 \\ C = \left(1-g^2\right)\left(f^2-g^2\right) - \mu f^2 g^2 - 4g\,\xi\xi_1 \\ D = g\left[2\xi\left(1-g^2-\mu g^2\right) + 2\xi_1\left(f^2-g^2\right)\right] \end{cases} \tag{3}$$

where $\mu = m_2 / m_1$ is the mass ratio, $\delta_{\mathrm{st}} = F_1 / k_1$ is the system static deformation, $\omega_{\mathrm{a}}^2 = k_2 / m_2$ is the square of the TMD intrinsic frequency, $\omega_{\mathrm{n}}^2 = k_1 / m_1$ is the square of the main system intrinsic frequency, $f = \omega_{\mathrm{a}} / \omega_{\mathrm{n}}$ is the intrinsic frequency ratio. $g = \omega / \omega_{\mathrm{n}}$ is the excitation frequency ratio, $c_{\mathrm{c}} = 2\sqrt{m_1 k_1}$ is the critical damping coefficient, $\xi = c_2 / c_{\mathrm{c}}$ is the TMD damping ratio, and $\xi_1 = c_1 / c_{\mathrm{e}}$ is the main system damping ratio.

3.1.2. Quantification of flutter uncertainty

In engineering, it is usually assumed that the chattering satisfies normal distribution. In order to quantify the effect of flutter uncertainty, a large number of samples of flutter are taken based on the Monte Carlo method, then the sampling results are subjected to flutter calculations, and finally the results are statistically analyzed in order to quantify the stability of the flutter of the bidirectional dense-ribbed cavity building cover. The structural response function is defined as:

$$R = R\left(H_i^*, A_i^*\right), i = 1,2,3,4 \tag{4}$$

Monte Carlo sampling and chattering analysis are carried out for the above functions as follows:

(1) Perform N sampling of the random variable $\left[H_i^*, A_i^*\right]^{\mathrm{T}}$ to obtain N vectors $\left[H_i^*, A_i^*\right]_j^{\mathrm{T}} (j = 1,2,\cdots,N)$ as samples.

(2) Input the N sets of sample vectors into the flutter calculation program, and then get the N corresponding responses, i.e., the N determined critical wind speeds for flutter.

(3) Statistically process the N flutter critical, when N is large enough, the stable statistics can be obtained, which are the mean ε, standard deviation σ and variance σ^2, and its calculation formula is:

$$\varepsilon = \left(x_1 + x_2 + x_3 + \cdots + x_N\right) / N \tag{5}$$

$$\sigma = \sqrt{\frac{\sum_{j=1}^{N}\left(x_j - \varepsilon\right)^2}{N}} \tag{6}$$

$$\sigma^2 = \frac{\sum_{j=1}^{N}\left(x_j - \varepsilon\right)^2}{N} \tag{7}$$

3.2. Optimized design of bi-directional dense ribbed cavity TMD parameters

3.2.1. TMD parameter optimization design

TMD, as a kind of vibration controller, can effectively control structural vibration in high-rise building structures. In order to solve the problem of structural fatigue caused by structural vibration due to chattering vibration of a two-way dense ribbed cavity building cover, a horizontal omnidirectional TMD device (HO-TMD) is proposed in this paper. This device mainly consists of a mass block, three sets of spring damping systems (one set on each side of the H-shaped slide rail) and two sets of slide rails. The lower slide is mounted on the internal flange of the dense ribbed cavity floor cover, and the mass block is mounted on the upper slide, which moves left and right along the slide, while the upper slide can be moved forward and backward along the lower slide, which can avoid the coupling effect of the spring during the bi-directional movement of the mass block, and make the bi-directional control accuracy of the damping system more accurate.

Fig. 2 shows the simplified working mechanical model of TMD on a bidirectional dense-ribbed cavity floor cover. In the figure, M is the mass of the two-way dense-ribbed cavity floor cover structure, x_M the horizontal displacement of the structure, C is the structural damping, K is the structural stiffness, k is the stiffness of the TMD damping device, m is the mass of the damping device, c is the damping device, $\mathbf{x}_{\mathrm{d}}$ is the displacement of the damping device, and $\mathbf{P}(t)$ is the wind load.

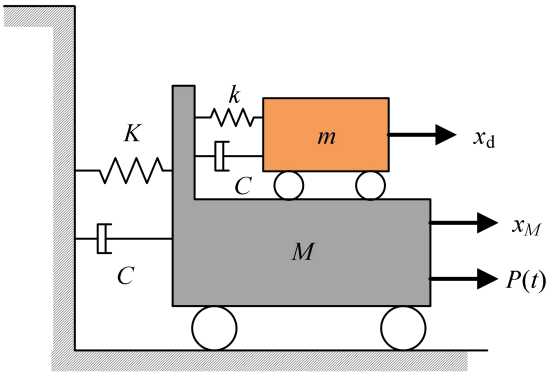

Figure 2. The empty chamber floor - TMD mechanical simplification model

The equations of motion for the system of two-way dense ribbed cavity floor cover vibration damping device are expressed as:

$$\begin{bmatrix} M & 0 \\ 0 & \mathrm{m} \end{bmatrix}\begin{bmatrix} \ddot{x}_M(t) \\ \ddot{x}_{\mathrm{d}}(t) \end{bmatrix}+\begin{bmatrix} C+c & -c \\ -c & c \end{bmatrix}\begin{bmatrix} \dot{x}_M(t) \\ \dot{x}_{\mathrm{d}}(t) \end{bmatrix}+\begin{bmatrix} K+k & -k \\ -k & k \end{bmatrix}\begin{bmatrix} x_M(t) \\ x_{\mathrm{d}}(t) \end{bmatrix}=\begin{bmatrix} P \\ 0 \end{bmatrix}\sin(\omega t) \tag{8}$$

Assuming a wind load of $Pe(t)$, the form of the solution to the above equation can be obtained as shown in the following equation:

$$\begin{bmatrix} \mathrm{x}_M(t) \\ \mathrm{x}_{\mathrm{d}}(t) \end{bmatrix}=\begin{bmatrix} x_M \\ x_{\mathrm{d}} \end{bmatrix}\mathrm{e}^{(\omega t)} \tag{9}$$

where x_M and x_{d} are the amplitude of vibration displacement of the structure and TMD, respectively.

Bringing Eq. (9) into Eq. (8) can be obtained:

$$\begin{bmatrix} x_M \\ x_{\mathrm{d}} \end{bmatrix}=\frac{1}{\det\left(K_{\mathrm{s}}-\omega^2 M_{\mathrm{s}}+\omega j C_{\mathrm{s}}\right)}\begin{bmatrix} \left(k-m\omega^2\right)+c\omega j & k+c\omega j \\ k+c\omega & \left(K+k-m\omega^2\right)+(C+c)\omega j \end{bmatrix}\begin{bmatrix} P \\ 0 \end{bmatrix} \tag{10}$$

where $K_{\mathrm{s}}, M_{\mathrm{s}}$ and C_{s} are the mass, stiffness and damping matrices of the system.

If the damping ratio of the main structure is assumed to be zero $\left(c_{\mathrm{p}}=0\right)$, according to Eq. (10),

the displacement amplification coefficient under dynamic loading after installation of the damping device can be found as:

$$R = \frac{x_M}{x_{\text{st}}} = \sqrt{\frac{\left(\alpha^2 - \beta^2\right)^2 + (2\xi\alpha\beta)^2}{\left[\left(\alpha^2 - \beta^2\right)\left(1 - \beta^2\right) - \alpha^2\beta^2\mu\right]^2 + (2\xi\alpha\beta)^2\left(1 - \beta^2 - \mu\beta^2\right)^2}} \tag{11}$$

Where x_{st} is the maximum static displacement of the system, $x_{\text{st}} = F / k_{\text{p}}$, ξ is the damping ratio $(\xi = c / 2m\omega)$ of the TMD, α is the ratio of the circular frequency of the TMD to that of the bidirectional dense-ribbed cavity floor cover structure. β is the ratio of the loading frequency to that of the bidirectional dense-ribbed cavity floor cover structure; μ is the mass ratio of the TMD, i.e., the ratio of the mass of the TMD mass block to the total mass of the bidirectional dense-ribbed cavity floor cover.

In order to optimize the control effectiveness of the TMD device on the bidirectional dense-ribbed cavity floor cover, the relationship between the parameters of the TMD device should be adjusted so as to minimize the amplification coefficient of the bidirectional dense-ribbed cavity floor cover structure, and thus to achieve the optimal control capability on the main structure. Different mass ratios μ are set in the calculations, whereby the optimal frequency ratios and the optimal damping ratios of the corresponding TMD devices are calculated. The calculation results are as follows:

$$\alpha_{\text{opt}} = \frac{1}{1 + \mu} \tag{12}$$

$$\xi_{\text{opt}} = \sqrt{\frac{3\mu}{8(1 + \mu)}} \tag{13}$$

where α_{opt} is the optimal frequency ratio of the TMD to the structural modes and ξ_{opt} is the optimal damping ratio of the TMD.

The mass, stiffness, and damping of the TMD device are calculated as follows:

$$\mathrm{k}_{\text{opt}} = \alpha_{\text{opt}}^2 \omega_1^2 m_d \tag{14}$$

$$c_{\text{opt}} = 2\xi_{\text{opt}}\alpha_{\text{opt}}\omega_1 m_{\text{d}} \tag{15}$$

$$m_{\text{d}} = \mu m_1 \tag{16}$$

where m_{d} is the mass of the TMD, k_{opt} is the stiffness of the TMD, C_{opt} is the damping of the TMD, ω_1 is the first-order circular frequency of the bi-directional dense-ribbed cavity floor structure, and m_1 is the first-order modal mass of the structure.

3.2.2. TMD Parameter Optimization Process

Based on the above process, the optimal design of TMD parameters considering flutter uncertainty can be carried out by combining Monte Carlo simulation and genetic algorithm, i.e., a large number of samples are generated using Monte Carlo sampling to simulate the flutter uncertainty, and on this basis, genetic algorithms are used for the whole-region search and optimization of TMD parameters. Under a given optimization objective, the TMD parameters that are the least sensitive to the effects of flutter uncertainty, i.e., the optimal TMD parameters, are searched. The optimization flow of TMD parameters under the condition of chattering uncertainty is shown in Fig. 3.

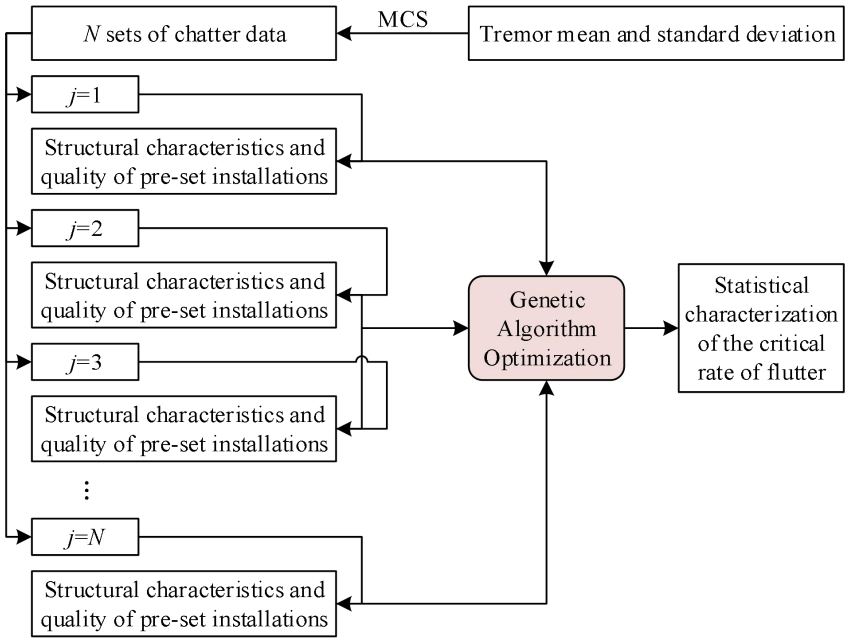

Figure 3. TMD parameter optimization process

(1) Based on the Monte Carlo method, random sampling of the flutter vibrations is carried out to generate N groups of representative flutter vibration samples, and these flutter vibrations are subjected to rational function fitting to generate the corresponding frequency-independent aerodynamic model parameters.

(2) For each group of aerodynamic model parameters and the given TMD parameters, carry out the calculation of the system flutter rate, and analyze the calculated N critical rates of flutter statistically, calculate the mean, variance and other statistics, and obtain the optimization target value.

(3) Combine the genetic algorithm to optimize the frequency and damping ratio of the TMD under the given optimization target, and obtain the final optimized design parameters of the TMD.

4. Calculation of performance and TMD parameters of two-way dense-ribbed cavity building cover

Currently, TMD is widely used in the vibration control of building structures, and the use of TMD technology for structural de-risking and strengthening is of great value in engineering applications. This chapter is mainly based on the two-way dense rib cavity building cover established by BIM technology to carry out TMD parameter optimization verification, aiming to further enhance the stability of the application of the two-way dense rib cavity building cover, and to improve the operational efficiency of the building on the basis of guaranteeing the safety of the building.

4.1. Performance analysis of bi-directional dense-ribbed cavity building cover

4.1.1. Experimental analysis of building deflection

In order to understand the stress state of the specimen, the stress change of the reinforcement inside the building cover, so as to derive the working condition of the two-way dense-ribbed cavity building cover, and due to the small span of the slab, only the surface of the reinforcement at the location of the cross-section in the middle of the span of the member is affixed with reinforcement strain gauges. Among them, A1~A7 were arranged to measure the deflection of the building cover, A3 was used to apply strain gauges in both longitudinal and transverse directions, A1, A4 and A7 were used to apply longitudinal strain gauges, and A2, A5 and A6 were used to apply transverse strain gauges.

Figure 4 shows the load deflection curves at each point inside the bidirectional dense-ribbed cavity building cover, of which Figures 4(a)~(b) are the load deflection curves at point A3 under uniform and concentrated loads, respectively, and Figures 4(c)~(d) are the deflection curves at each point under concentrated load and the deflection curves under the internal X-direction concentrated loads, respectively.

The test results show that the deflection value in the plate is 0.588mm when the uniform load is 6kN/m^2 and 2.216mm when the concentrated load is 30kN/m^2.According to the figure, it can be found that the three geometrically symmetrical measurement points, points A1 and A5, points A2 and A4, and points A6 and A7, the load-deflection curves are almost overlapped, which indicates that when subjected to the action of concentrated load, the force and deflection are also symmetric. When the support deflection is zero, the deflection of each measurement point in the plate can be calculated according to the interpolation method. The deflection of each point in the two-way dense-ribbed cavity floor cover under concentrated load can be calculated, as shown in Fig. 4(d). Some studies have proposed a quadratic parabolic relationship between the maximum deflection and the load approximately in the experimental study of a quadratically supported continuous two-way dense-ribbed floor cover. The quadratic parabola with the deflection value at point A3 as the vertex was adopted as the ideal curve, which was compared with the test measured curve. According to the measured deflection, it can be calculated that under the action of 25kN/m^2 centralized load, the deflection in the X and Y directions of point A3 in the two-way cavity building cover is 1.218mm and 1.237mm respectively, and under the action of 30kN/m^2 centralized load, the deflection in the X and Y directions of point A3 in the building cover is 1.531mm and 1.569mm respectively, and the deflection in the two-way cavity building cover is 1.531mm and 1.569mm in both directions. The deflections of the building cover in the two directions basically coincide with each other, which is a good indication of its good structural performance and strong bi-directionality.

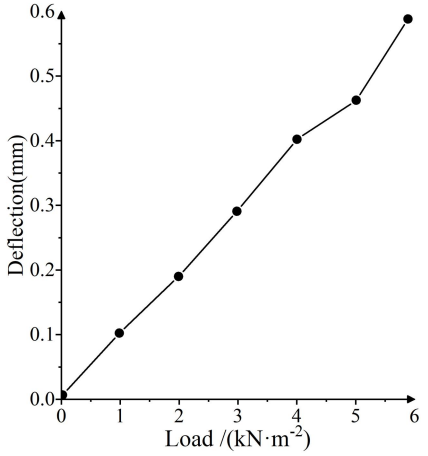

(a) Uniform load A3

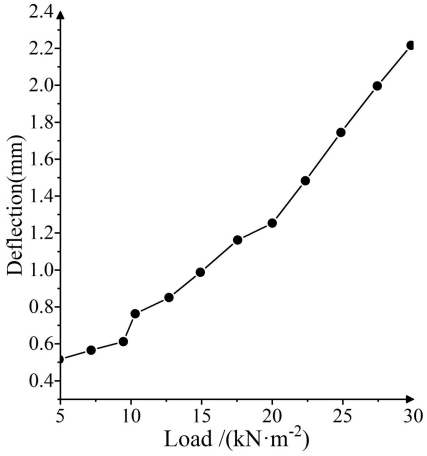

(b) Concentrated load A3

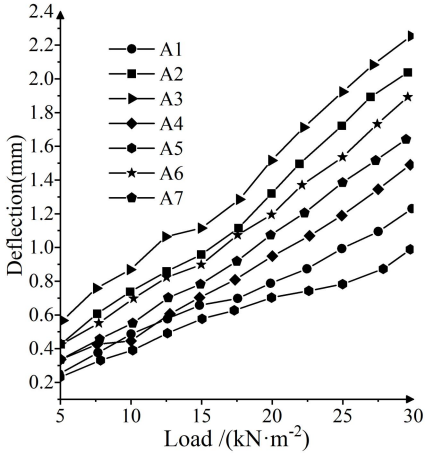

(c) Deflection of loads at each internal point

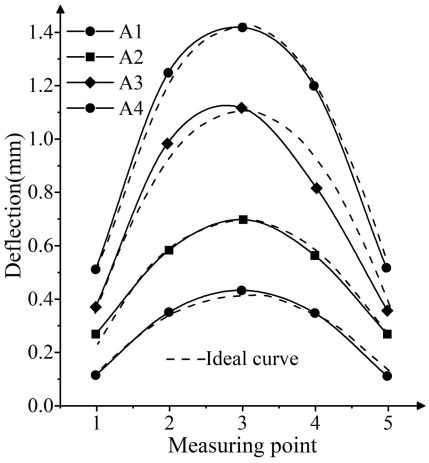

(d) The x-direction inside the board

Figure 4. Load deflection curve

4.1.2. Comparison of the performance of different building covers

For comparison, the cavity of the finite element model of the two-way dense-ribbed cavity floor cover is filled, which becomes the finite element model of the flat slab without beams, and the bottom and top plates of the hollow box are removed, which becomes the finite element model of the cross

beams. Finite element analysis of the above two floor cover forms are carried out separately, and the loads and constraints are the same as those of the bidirectional dense-ribbed cavity floor cover.

For the two-way dense-ribbed cavity floor cover (KQ) and the flat slab without beam (PB), we apply a face load of 5kN/m^2, and for the crossbeam floor cover (JC), in order to simplify it, we simplify the face load into a centralized load that is all concentrated at the rib-beam intersections, 12 nodes at the intersection of the intermediate ribs and beams, with an input centralized load of 2.5kN at each node, and 1 node in the corners, with an input centralized load of 0.5kN at each node. The centralized load is 0.5kN, 4 nodes at the intersection of the edge beams and intermediate beams, and the centralized load input at each node is 1.5kN. The deflection and bending moment of the three building cover forms are compared respectively, and the comparison results are shown in Table 1.

As can be seen from the table, the mid-span deflection of the two-way dense-ribbed cavity floor cover with limited distance is 0.814 mm, which is slightly larger than the mid-span deflection of the flat slab-on-grade floor cover (0.581 mm), and a lot smaller than the mid-span deflection of the cross-beam floor cover (4.589 mm), which is about one-fifth of the mid-span deflection of the cross-beam floor cover. In addition, the mid-span moment of the two-way dense-ribbed hollow-cavity floor cover is slightly larger than that of the flat slab without beams, and much smaller than that of the cross-beam floor cover. This is mainly due to the role of the hollow box, the hollow box of the upper and lower plate can be regarded as the wing edge of the rib, under the action of the load can share a part of the moment, that is, the hollow box can improve the force performance of the building cover. It can be seen that the hollow box and cast-in-place dense-ribbed cavity floor cover has a better common role, in the calculation of two-way dense-ribbed cavity floor cover deflection, must consider the role of the hollow box, otherwise it may cause a large error. Then, the underestimation of the stiffness of the two-way dense-ribbed cavity floor cover may have an impact on clarifying the vibration characteristics of the two-way dense-ribbed cavity floor cover.

Table 1. Comparison results of different building models

Coordinates	Deflection (mm)			Bending moment (kN·m)		
	PB	JC	KQ	PB	JC	KQ
(3.028,0.873)	0.243	1.836	0.311	2.972	16.963	5.028
(3.028,1.467)	0.426	3.251	0.602	4.486	31.514	7.103
(3.028,2.338)	0.537	4.164	0.756	5.215	40.487	8.112
(3.028,3.028)	0.581	4.589	0.814	5.439	49.605	8.386

4.2. Validation analysis of TMD parameter optimization algorithms

4.2.1. Comparison of chatter control performance

Relying on the bidirectional dense-ribbed cavity building cover model established by BIM technology, combined with the TMD vibration model for vibration damping, the TMD parameter optimization design method is utilized, aiming to achieve vibration damping and stabilization of the bidirectional dense-ribbed cavity building cover. In order to verify the chattering vibration control performance of HO-TMD, two traditional parameter optimization methods are used as comparisons (A and B) to optimize the design of the TMD parameters under different mass ratios, respectively, and the optimal TMD parameters are obtained as shown in Table 2.

From the data in the table, it can be seen that the optimal damping of the TMD obtained by the HO-TMD method is smaller than the optimal damping obtained by the two traditional methods. This is because the traditional parameter optimization design method adopts the structural eigenfrequency to design the TMD, and due to the influence of aerodynamic damping and stiffness, the actual vibration frequency of the structure will change when the flutter vibration occurs, and the adoption of the eigenfrequency for the design of the TMD can not take into account the influence of the aerodynamic damping and stiffness effects.

Table 2. TMD optimum parameters obtained by different methods

Mass ratio	Optimize parameters	Method A	Method B	Ours
0.06	k_{opt}	0.9851	0.9763	0.8329
	C_{opt}	0.0742	0.0735	0.0563
0.12	k_{opt}	0.9751	0.9806	0.8158
	C_{opt}	0.1065	0.1023	0.0862
0.18	k_{opt}	0.9871	0.9796	0.8157
	C_{opt}	0.1238	0.1128	0.0733
0.24	k_{opt}	0.9814	0.9785	0.8018
	C_{opt}	0.1451	0.1427	0.0862

In order to compare the flutter control performance of the TMDs designed by different methods on the original structure, the flutter control efficiency is defined as $\eta = (K_t - K)/K * 100\%$, where K and K_t denote the critical rate of structural flutter without and with TMDs, respectively. The flutter control frequencies of the bidirectional dense-ribbed cavity building cover obtained by different methods are shown in Fig. 5.

From the figure, it can be seen that the TMD chattering control efficiencies obtained by the HO-TMD parameter optimization design method proposed in the article are all significantly higher than those of the two comparative methods, thus verifying the aforementioned conclusion that neglecting the effects of aerodynamic damping and stiffness will result in the TMD not being able to exert optimal control performance. In addition, with the increase of mass ratio, the TMD chattering control efficiencies obtained by the three TMD parameter design methods are all getting higher and higher. Among them, the two-way dense-ribbed cavity building-TMD system obtained by the method of this paper has the best flutter control effect, with a flutter control efficiency of up to 45.15%, and its growth with mass ratio is also the largest.

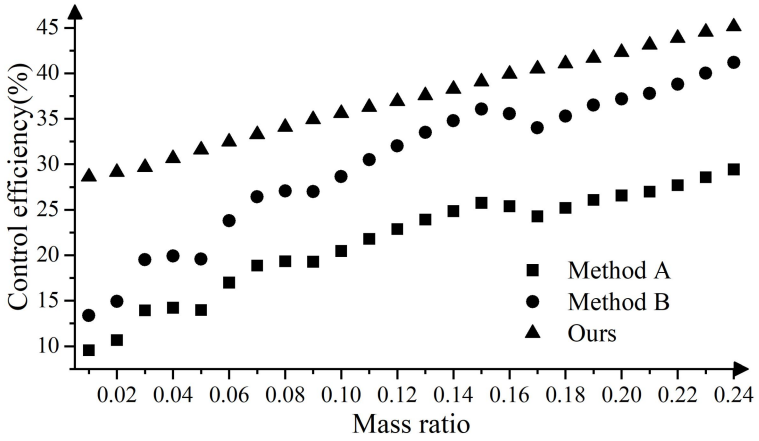

Figure 5. Flutter control efficiency obtained by different methods

4.2.2. Vibration damping for different loads

To further analyze the vibration damping performance of HO-TMD, the mass ratio of the damper was set to 0.24. In terms of loading, considering that the two-way dense-ribbed cavity building cover may be searched for wind excitation during the application process, two working conditions with different wind speeds were set up, with the wind speeds of GK1 and GK2 being 5m/s and 10m/s, respectively, to analyze the vibration damping effects of HO-TMD and TMD under the action of loads with different wind speeds. The Fig. 6 shows the vibration damping under different loading conditions, where Fig. 6(a)~(b) shows the longitudinal rocking response of GK1 and GK2, and Fig. 6(c)~(d) shows the longitudinal rocking power spectra of GK1 and GK2, respectively.

As can be seen from the figure, since the dominant frequency of the response of Case 1 is the peak frequency of the wind speed excitation, the frequency misalignment leads to the deterioration of the TMD damping effect, and the longitudinal root-mean-square (RMS) damping rate is only 0.18%, which

is almost unchanged, and there is even a negative effect of increasing the response in part of the time period, whereas, the proposed HO-TMD is able to track this frequency change and realize the active frequency tuning, and the longitudinal root-mean-square (RMS) damping rate is 15.37%, which is obviously superior to the traditional TMD method. This is also evident from the comparison of the response power spectra in Fig. 6(c). In Case 2, the peak wind speed frequency is close to the longitudinal vibration frequency, and the resonance response is obvious. At this time, the longitudinal RMS damping rates of TMD and HO-TMD for the bidirectional dense-ribbed cavity building are 21.58% and 16.79%, respectively, and TMD plays a better vibration damping role because of the non-dislocated frequency. The HO-TMD is slightly lower than the TMD in vibration damping effect due to the limitation of the vibrator displacement by the baffle plate. Taken together, the horizontal omni-directional TMD designed in this paper has a better performance in ensuring the stability of the bi-directional dense-ribbed cavity building cover, and in the additional frequency tracking, it is further clarified that the HO-TMD has an obvious tuning advantage. This also fully demonstrates that the model of bidirectional dense-ribbed cavity building cover designed by BIM technology helps to better grasp the relevant performance of bidirectional dense-ribbed cavity building cover, and lays the foundation for improving the vibration-damping stability of bidirectional dense-ribbed cavity building cover.

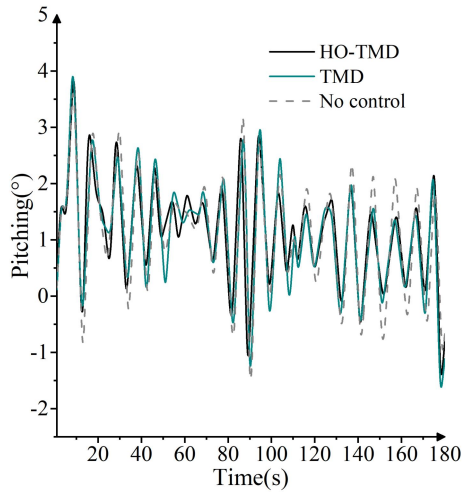

(a) Pitch response - GK1

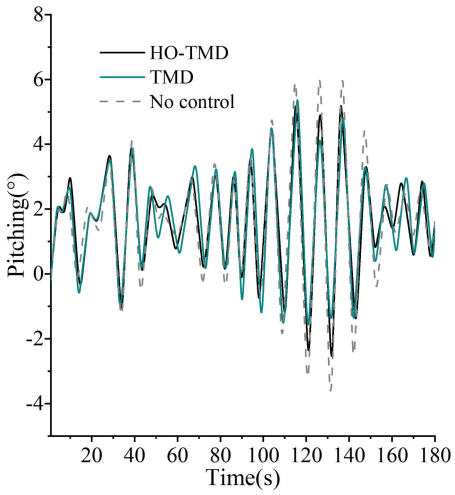

(b) Pitch response - GK2

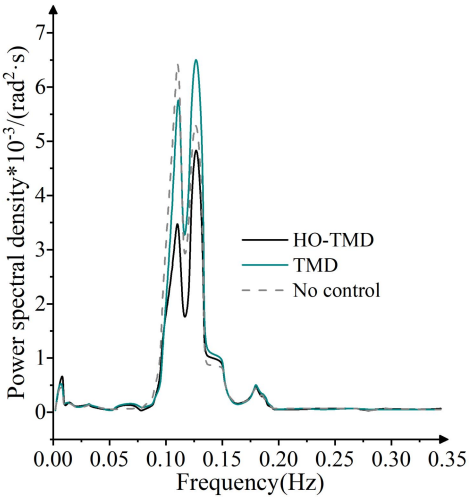

(c) Pitch power spectrum - GK1

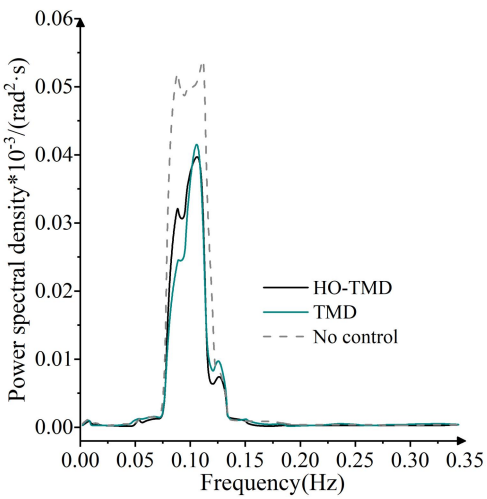

(d) Pitch power spectrum – GK2

Figure 6. Vibration reduction under different load cases

4.2.3. Changes in the displacement response of the building cover

On the basis of clarifying the vibration damping control effect of HO-TMD on two-way dense-ribbed cavity building cover, this paper further explores the trend of displacement response of two-way dense-ribbed cavity building cover under different stiffness and damping. Figure 7 shows the

contour plots of the standard deviation of the displacement response of the bidirectional dense-ribbed cavity building cover, in which Figures 7(a)~(b) show the standard deviation of the displacement response in the longitudinal and lateral directions, respectively. The darker color in the plots represents the smaller standard deviation of displacement for two-way dense-ribbed cavity building cover, and the better vibration damping effect.

Comparing the standard deviation of displacement response in the longitudinal and lateral directions, it can be seen that the robustness of HO-TMD in the X direction is obviously better than that in the Y direction, and when the HO-TMD parameters deviate from the optimal stiffness and damping in the X direction, a better control effect can still be obtained. On the contrary, at low stiffness and damping in the Y direction, multiple local optima appear near the global optima. While the surface is smoother at higher stiffness and damping. Obviously, this is caused by the fact that the oscillator is more likely to collide with the limiting device at lower stiffness and damping. This also shows that it is feasible to use the parametric design optimization solution algorithm designed in this paper.

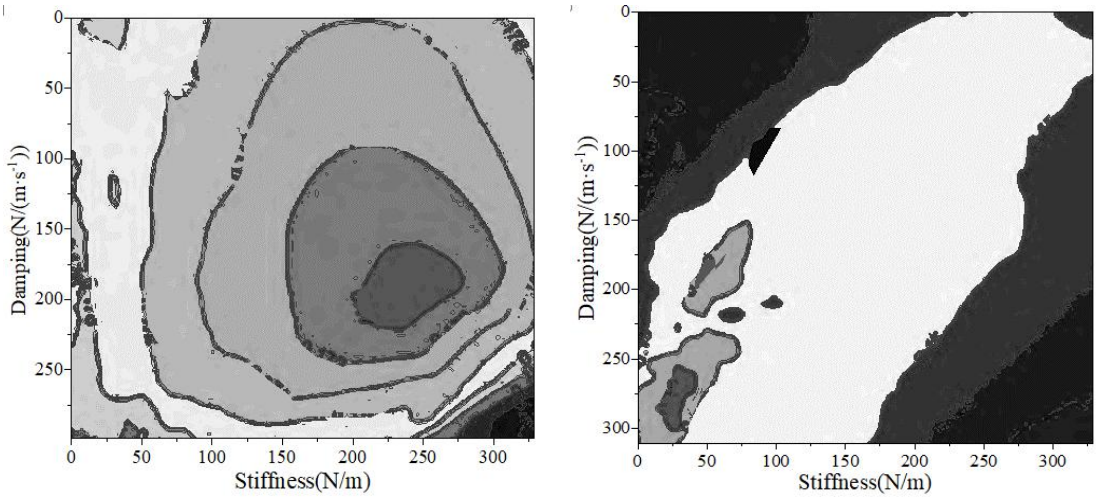

(a) Longitudinal (b) Side direction

Figure 7. Contour map of standard deviation of displacement response

For the vibration damping effect of two-way dense ribbed cavity building cover in practical application, this paper further discusses the displacement of the building cover under different combinations of the number of TMDs. A total of five combinations of TMD numbers (1, 3, 5, 7, 9 units) are set up to compare the vibration damping rate of the bidirectional ribbed cavity building with different combinations of TMD numbers. In the previously designed two-way dense ribbed cavity building model, several nodes (P1~P7) are set up, and the node displacements of the two-way dense ribbed cavity building with different TMD combinations are obtained at a disturbance frequency of 1.5 Hz, as shown in Table 3.

From the table, it can be seen that TMD can significantly suppress the structural vibration of two-way dense-ribbed cavity floor cover under different installation conditions, and the effect varies according to the combination of conditions. The finite element analysis shows that the installation of 3 TMDs can make the roof vibration reduction effect reach 39.41%. When the number of TMDs is increased to 5, the vibration damping effect can be further improved to 51.17%. This result shows that as the number of TMDs increases, the overall vibration damping effect is improved, although the mass of individual devices is reduced accordingly. As the number of TMDs continues to increase, the mass of individual TMDs is further reduced, which may lead to a weakening of their control ability and hence a reduction in the vibration damping effect. For example, Case 4 and Case 5 reduce the vibration response by 8.36% and 13.51%, respectively, indicating that increasing the number of TMDs does not always improve the vibration damping effect. An increase in the number of TMD installations can expand the vibration control range and improve the vibration damping effect, but this effect does not grow linearly, and the damping effect decreases after exceeding a certain value.

Through comparative analysis, it can be found that 3 and 5 TMDs have relatively the best damping effect. This may be due to the most reasonable configuration of TMDs in these two working conditions, which ensures sufficient control capacity and avoids the problem of too small mass of individual devices. Therefore, in practical applications, choosing the right number and configuration of TMDs is crucial to achieve the best vibration damping effect.

Table 3. Displacement of floor slab nodes

-	TMD-1	TMD-3	TMD-5	TMD-7	TMD-9
P1	0.715	0.427	0.335	0.627	0.617
P2	0.711	0.436	0.352	0.663	0.626
P3	0.583	0.381	0.307	0.528	0.524
P4	0.414	0.292	0.218	0.403	0.383
P5	0.428	0.283	0.224	0.416	0.406
P6	0.315	0.215	0.165	0.297	0.289
P7	0.298	0.196	0.153	0.293	0.275
Peak value (mm)	0.739	0.453	0.363	0.675	0.632
Damping ratio (%)	-	39.41	51.17	8.36	13.51

In summary, in the actual application process of two-way dense ribbed cavity building cover, BIM technology should be fully combined to simulate the impact of different combinations of TMD on the vibration damping effect of the building cover in order to accurately grasp the stability of the two-way dense ribbed cavity building cover. Comprehensive consideration of various factors to determine the most suitable TMD installation program and quantity, in order to enhance the operational effect of building construction and building safety to lay a solid foundation.

5. Conclusion

The article combines BIM technology with TMD parameter optimization, proposes a horizontal omnidirectional TMD parameter optimization design method, and carries out verification analysis through examples. Based on the experimental results, it is clear that the horizontal omnidirectional TMD can rely on the simulation model constructed by BIM technology for parameter optimization, and the results obtained are in line with the building requirements of bidirectional dense-ribbed cavity building, which can help to improve the operational efficiency of the building on the basis of ensuring the safety and stability of the building construction. To a certain extent, the research in this paper provides a new research vision for the coordinated application of BIM technology and TMD, and also provides theoretical support to ensure the vibration damping effect of bidirectional dense-ribbed cavity building cover.

The article still has some deficiencies while obtaining the research results. For example, when carrying out the design of the bidirectional dense-ribbed cavity building cover model, only the main structure was considered without further designing the prestressing reinforcement model of the building cover, which may lead to the exacerbation of vibration frequency of the building cover under external loading, thus having an impact on the TMD parameters. In the subsequent study, the possible influence of prestressing of the two-way dense ribbed cavity building cover will be further considered, and the optimal design method of TMD parameters will be further improved to fully ensure the stability of the two-way dense ribbed cavity building cover.

Funding

This research was supported by the 2019 Hubei Provincial Department of Education Science and Technology Research Project Provincial Key Project: “Research on TMD Collision Vibration Reduction Based on Bidirectional Multi ribbed Hollow Floor” (B2019399).

References

1. Gong, L., Feng, Y., Zhang, W., Xu, M., & Zeng, X. (2025). Vibration Performances of a Full-Scale Assembled Integral Two-Way Multi-Ribbed Composite Floor. Buildings, 15(9), 1551.
2. Jiang, Y., Liu, L., Wang, X., Liu, R., & Yang, H. (2025). Study on Bending Performance of High-Ductility Composite Slab Floor with Composite Ribs. Materials, 18(3), 658.
3. Li, X., Zhang, C., An, R., & Zhu, H. (2025, October). Flexural behavior of a new type of hollow concrete composite slab. In Structures (Vol. 80, p. 109920). Elsevier.
4. Luo, B., Tang, Z., Zhao, F., Song, Y., & Cao, G. (2025). Experimental investigation of the Bending Behavior of Ribbed Composite Slabs with UHPC Liner. Case Studies in Construction Materials, e05260.
5. Vejrum, P., & Jensen, M. S. (2022). Design and construction of a ribbed concrete slab based on isostatic lines.

In Structures and Architecture. A Viable Urban Perspective? (pp. 1247-1254). CRC Press.
6. Gamal, M., Heiza, K., Hekal, G. M., & Nabil, A. (2023, March). Voided slabs as a new construction technology-a review. In Proceedngs of the International Conference on Advances in Structural and Geotechnical Engineering, ICASGE (Vol. 23).
7. Shepelev, A. P., Ibatullin, R. R., & Pischulev, A. A. (2025). An improved precast reinforced concrete multi-cavity floor slab of aggregate-flow production technology. The results of full-scale loading tests. Urban construction and architecture, 15(2), 12-20.
8. Li, C., Li, G., Yu, R., Ma, X., Qin, P., & Wang, X. (2020). Study on Mechanical Properties of Multi-Cavity Steel–Concrete Composite Floor. Applied Sciences, 10(23), 8444.
9. Safar, A., & Lou, K. B. (2007). A study of the action of the beam and beamless (flush) floor slabs of the multistorey buildings. Erciyes Üniversitesi Fen Bilimleri Enstitüsü Fen Bilimleri Dergisi, 23(1), 127-135.
10. Wang, D., & Li, J. (2020, February). Experimental Analysis and Research on New Concrete Multi-ribbed Beam Hollow Floor. In IOP Conference Series: Earth and Environmental Science (Vol. 446, No. 2, p. 022040). IOP Publishing.
11. Zeng, X., Feng, Y., Ruan, S., Xu, M., & Gong, L. (2023). Experimental and Numerical Study on Flexural Behavior of a Full-Scale Assembled Integral Two-Way Multi-Ribbed Composite Floor System. Buildings, 13(10), 2517.
12. Ma, J., Gomaa, M., Bao, D. W., Javan, A. R., & Xie, Y. M. (2022). PrintNervi–Design and construction of a ribbed floor system in the digital era. Journal of the International Association for Shell and Spatial Structures, 63(4), 241-251.
13. Huang, Y., Yang, J., & Zhong, C. (2022). Flexural performance of assembly integral floor structure voided with steel mesh boxes. Journal of Building Engineering, 54, 104693.
14. Bosbach, S., Kalthoff, M., Morales Cruz, C., Adam, V., Matschei, T., & Classen, M. (2023). Digital Prefabrication of Lightweight Building Elements for Circular Economy: Material-Minimised Ribbed Floor Slabs Made of Extruded Carbon Reinforced Concrete (ExCRC). Buildings, 13(12), 2928.
15. Souza, C. F. N., Pacheco, F., Oliveira, M. F., Heissler, R. F., & Tutikian, B. F. (2020). Impact sound insulation of floor systems with hollow brick slabs. Case Studies in Construction Materials, 13, e00387.
16. Mata-Falcón, J., Bischof, P., Huber, T., Anton, A., Burger, J., Ranaudo, F., ... & Kaufmann, W. (2022). Digitally fabricated ribbed concrete floor slabs: a sustainable solution for construction. RILEM Technical Letters, 7, 68-78.
17. Chen, X., & Ma, Q. (2024). Experimental study on the flexural performance of concrete hollow composite slabs with tightly connected panel sides. Scientific Reports, 14(1), 20784.
18. Jin, J., Hu, W., Zheng, F., & Wu, B. (2025). Experimental and Numerical Studies on the Mechanical Behavior of a Novel Bidirectional, Prestressed, Prefabricated, Composite Hollow-Core Slab. Buildings, 15(2), 232.
19. Zhang, Z., Chen, F., Yu, W., Sheng, J., Wei, L., & Hu, A. (2025). Mechanical Performance of Square Box-Type Core Mold Hollow Floor Slabs Based on Field Tests and Numerical Simulation. Buildings, 15(16), 2948.
20. Engle, T., Mahmoud, H., & Chulahwat, A. (2015). Hybrid tuned mass damper and isolation floor slab system optimized for vibration control. Journal of Earthquake Engineering, 19(8), 1197-1221.
21. Wang, L., Shi, W., Zhang, Q., & Zhou, Y. (2020). Study on adaptive-passive multiple tuned mass damper with variable mass for a large-span floor structure. Engineering Structures, 209, 110010.
22. Islam, B., & Ahsan, R. (2012, September). Optimization of tuned mass damper parameters using evolutionary operation algorithm. In 15th World Conference in Earthquake Engineering.
23. Farshidianfar, A., & Soheili, S. (2013). ABC optimization of TMD parameters for tall buildings with soil structure interaction. Interact Multiscale Mech, 6(4), 339-356.
24. Kamgar, R., Samea, P., & Khatibinia, M. (2018). Optimizing parameters of tuned mass damper subjected to critical earthquake. The Structural Design of Tall and Special Buildings, 27(7), e1460.
25. Kaveh, A., Javadi, S. M., & Moghanni, R. M. (2020, December). Optimal structural control of tall buildings using tuned mass dampers via chaotic optimization algorithm. In Structures (Vol. 28, pp. 2704-2713). Elsevier.
26. Djedoui, N., & Ounis, A. (2022). Optimization of TMD parameters in frequency domain including SSI effect by means of recent metaheuristic algorithms. Practice Periodical on Structural Design and Construction, 27(3), 04022026.
27. Suryadi, D., Prasetya, A., Daratha, N., & Agustian, I. (2023). Optimum design of tuned mass damper parameters to reduce seismic response on structure using genetic algorithm. ASEAN Engineering Journal, 13(1), 41-49.
28. Yang, X., Lei, Y., Wang, J., Zhu, H., & Shen, W. (2023). Physics-enhanced machine learning-based optimization of tuned mass damper parameters for seismically-excited buildings. Engineering Structures, 292, 116379.
29. Yu Luo,Yiminxuan Liu,Xiaofeng Liao,Changsaar Chai,Heap Yih Chong,Yongtong Huang & Zhaoyin Zhou. (2025). Optimizing Reinforcement Bar Fabrication in Construction Projects via Multi-Dimensional Applications in Building Information Modeling. Applied Sciences,15(19),10807-10807. https://doi.org/10.3390/APP151910807.
30. Abbaspour Atefeh,Yousefi Hossein,Aslani Alireza & Noorollahi Younes. (2022). Economic and Environmental Analysis of Incorporating Geothermal District Heating System Combined with Radiant Floor Heating for Building Heat Supply in Sarein, Iran Using Building Information Modeling (BIM). Energies,

15(23), 8914-8914.https://doi.org/10.3390/EN15238914.
31. Jianyong Chen. (2025). Research on TMD collision damping based on two-way dense ribbed cavity building cover. Applied Mathematics and Nonlinear Sciences,10(1),https://doi.org/10.2478/AMNS-2025-0652.